Acta Biochimica Polonica

Vol. 54 No. 1/2007, 183–192

on-line at: www.actabp.pl

Regular paper

The role of alkyl chain length in the inhibitory effect n-alkyl xanthates on mushroom tyrosinase activities

Ali Akbar Saboury[1]✉, Mahdi Alijanianzadeh[1] and Hasan Mansoori-Torshizi[2]

[1]*Institute of Biochemistry and Biophysics, University of Tehran, Tehran, Iran;* [2]*Department of Chemistry, University of Sistan and Baluchestan, Zahedan, Iran*

Received: 27 December, 2006; revised: 03 March, 2007; accepted: 12 March, 2007
available on-line: 20 March, 2007

Sodium salts of four n-alkyl xanthate compounds, $C_2H_5OCS_2Na$ (I), $C_3H_7OCS_2Na$ (II), $C_4H_9OCS_2Na$ (III), and $C_6H_{13}OCS_2Na$ (IV) were synthesized and examined for inhibition of both cresolase and catecholase activities of mushroom tyrosinase (MT) in 10 mM sodium phosphate buffer, pH 6.8, at 293 K using UV spectrophotemetry. 4-[(4-methylbenzo)azo]-1,2-benzendiol (MeBACat) and 4-[(4-methylphenyl)azo]-phenol (MePAPh) were used as synthetic substrates for the enzyme for catecholase and cresolase reactions, respectively. Lineweaver-Burk plots showed different patterns of mixed, competitive or uncompetitive inhibition for the four xanthates. For the cresolase activity, I and II showed uncompetitive inhibition but III and IV showed competitive inhibition pattern. For the catecholase activity, I and II showed mixed inhibition but III and IV showed competitive inhibition. The synthesized compounds can be classified as potent inhibitors of MT due to their K_i values of 13.8, 11, 8 and 5 μM for the cresolase activity, and 1.4, 5, 13 and 25 μM for the catecholase activity for I, II, III and IV, respectively. For the catecholase activity both substrate and inhibitor can be bound to the enzyme with negative cooperativity between the binding sites (α>1) and this negative cooperativity increases with increasing length of the aliphatic tail of these compounds. The length of the hydrophobic tail of the xanthates has a stronger effect on the K_i values for catecholase inhibition than for cresolase inhibition. Increasing the length of the hydrophobic tail leads to a decrease of the K_i values for cresolase inhibition and an increase of the K_i values for catecholase inhibition.

Keywords: mushroom tyrosinase, alkyl xanthate, mixed inhibition, competitive inhibition, uncompetitive inhibition, inhibition constant

INTRODUCTION

Tyrosinase (EC.1.14.18.1), also known as polyphenol oxidase, is a copper-containing multifunctional oxidase that catalyzes both the hydroxylation of monophenols to diphenols and the oxidation of *o*-diphenols to *o*-quinones. Tyrosinase is common in plants and animals and is involved in the formation of melanin pigments (Pawelek & Korner, 1982; Zawistowski *et al.*, 1991; Chen & Kubo, 2002). In the food industry, tyrosinase is a very important enzyme in controlling the quality and economics of fruit and vegetable storage and processing, including fruit pulp manufacturing (Whitaker, 1995; Lee, 2002). Tyrosinase catalyzes the oxidation of phenolic compounds to the corresponding quinones and is responsible for the enzymatic browning of fruits and vegetables. In addition to the undesirable color and flavor, the quinone compounds produced in the browning reaction may irreversibly react with the amino and sulfhydryl groups of proteins. The quinone–protein reaction decreases the digestibility of the protein and the bioavailability of the essential amino acids including lysine and cysteine. Tyrosinase inhibition may be a potential approach to prevent and control the enzymatic browning reactions

✉Correspondence to: A. A. Saboury, Institute of Biochemistry and Biophysics, University of Tehran, Tehran, Iran; tel: (98 21) 6695 6984; fax: (98 21) 6640 4680; e-mail: saboury@ut.ac.ir

Abbreviation: MeBaCat, 4-[(4-methylbenzo)azo]-1,2-benzendiol; MePAPh, 4-[(4-methylphenyl)azo]-phenol; MT, mushroom tyrosinase; K_m', apparent Michaelis constant; V_{max}', apparent maximum velocity; K_i, inhibition constant.

and improve the quality and nutritional value of food products (Liangli, 2003). Tyrosinase also plays an important role in the developmental and defensive functions of insects. Tyrosinase is involved in melanogenesis, wound healing, parasite encapsulation, and sclerotization in insects (Lee *et al.*, 2000; Sugumaran, 1988; Barrett, 1984).

Recently, the development of tyrosinase inhibitors has become an active alternative approach to control insect pests (Liangli, 2003). In addition, it is well-recognized that tyrosinase inhibitors are important for their potential applications in medical and cosmetic products that may be used to prevent or treat pigmentation disorders (Pawelek & Korner, 1982; Mosher *et al.*, 1983; Maeda & Fukuda, 1991). Tyrosinase inhibitors may result in a reduction in melanin biosynthesis and are used in cosmetic products for perpigmentation-related concerns, including the formation of freckles (Liangli, 2003). Tyrosinase may also be a target for developing medicines to treat hypopigmentation-related problems, such as albinism and piebaldism (Pawelek & Korner, 1982). Other biological functions of tyrosinase include neuromelanin formation in human brain and the melanoma specific anticarcinogenic activity (Chen & Kubo, 2002). Recent research indicated that tyrosinase could play a role in dopamine neurotoxicity and contribute to the neurodegeneration associated with Parkinson's disease (Xu *et al.*, 1997). In the mushroom (*Agaricus bisporus*), as well as in fruits and vegetables, the enzyme is responsible for browning, a commercially undesirable phenomenon (Martinez & Whitaker, 1995; Whitaker, 1995; Xie *et al.*, 2003). Tyrosinase (MT) from *A. bisporus*, with a molecular mass of 120 kDa, is composed of two H subunits (43 kDa) and two L subunits (13 kDa) and contains two active sites (Strothkemp *et al.*, 1976; Yong *et al.*, 1990). Chemical and spectroscopic studies of tyrosinase have demonstrated that the geometric and electronic structures of the binuclear copper active site of this enzyme are extremely similar to those found in hemocyanins (Schoot, 1972; Hepp *et al.*, 1979; Himmelwright *et al.*, 1980). In the formation of melanin pigments, three types of tyrosinase (met, oxy and deoxytyrosinase) with different binuclear copper structure of the active site are involved (Lerch, 1981; Wilcox *et al.*, 1985; Sanchez-Ferrer *et al.*, 1995). Mettyrosinase, the resting form of tyrosinase, contains two tetragonal Cu(II) ions antiferromagnetically coupled through an endogenous bridge, although hydroxide exogenous ligands other than peroxide are bound to the copper site (Himmelwright *et al.*, 1979). This species can be converted by addition of peroxide to oxytyrosinase, which decays back to mettyrosinase when the peroxide is lost. Oxytyrosinase can also be produced by the two-electron reduction of deoxytyrosinase, followed by the reversible binding of dioxygen (Himmelwright *et al.*, 1980), which reacts with monophenol as well as *o*-diphenol substrate. Oxytyrosinase contains two tetragonal Cu(II) atoms, each coordinated by two strong equatorial and one weaker axial N_{His} ligands. An exogenous oxygen molecule is bound as peroxide and bridges the two copper centers (Wilcox *et al.*, 1985; Kim *et al.*, 2004). Deoxytyrosinase, an analogue of deoxyhemocyanin, has a bicuprous structure [(Cu(I)-Cu(I)].

Tyrosinase has three domains, of which the central one contains two copper binding sites. Six histidine residues bind a pair of copper ions in the active site of tyrosinase, which interact with both molecular oxygen and its phenolic substrate (Jackman *et al.*, 1991). A vast variety of natural and synthetic inhibitors are known against the catecholase, cresolase or both activities of tyrosinase. Polyphenols, aldehydes and their derivatives are the most important inhibitors from plant natural sources (Kubo & Kinst-Hori, 1988; 1999; Kubo *et al.*, 1994; 2000). Besides higher plants, some compounds from fungal sources have also been identified, e.g. metallothionein from *Aspergillus niger* has a strong avidity to chelate copper at the active site of MT, thereby acting as a strong inhibitor (Goetghebeur & Kermasha, 1996). Kojic acid, an antibiotic, produced by species of *Aspergillus* and *Penicillum* in an aerobic process acts as a potent, "slow-binding", competitive inhibitor of tyrosinase (Chen *et al.*, 1991; Kahn, 1995; Kahn *et al.*, 1997; Kim *et al.*, 2002), and is widely used as a cosmetic whitening agent (Cabanes *et al.*, 1994; Kahn *et al.*, 1997; Lim, 1999; Battaini *et al.*, 2000). Synthetic tyrosinase inhibitors may be used as drugs and chemicals. In the case of clinical drugs, captopril, an antihypertensive drug, and methimazole act as tyrosinase inhibitors (Andrawis & Khan, 1996; Espin & Wichers, 2001). Simple chemical species capable of binding to copper, such as cyanide, azide, and halide ions, as expected behave as purely competitive inhibitors towards dioxygen binding, although strong differences have been seen among polyphenoloxidases from different sources (Ferrar & Walker, 1996). Sulfur-containing compounds such as tiron, thiol and sulfites are among the most important tyrosinase inhibitors. Currently, the most commonly applied inhibitor of the discoloration process is sulfite (Taylor & Bush, 1986).

To understand the mechanism of enzyme action and inhibition, we have attempted to obtain additional information about the structure, function and relationships of MT (Karbassi *et al.*, 2003; 2004; Haghbeen *et al.*, 2004; Shareefi *et al.*, 2004; Gheibi *et al.*, 2005). After introducing two new bi-pyridine synthetic compounds as potent uncompetitive MT inhibitors (Karbassi *et al.*, 2004), the inhibitory effects of three synthetic n-alkyl dithiocarbamates, with different tails, were elucidated (Gheibi *et al.*, 2004). The

binding process for catecholase inhibition by benzenethiol showed the predominant hydrophobic interaction in the active site of the enzyme, while an electrostatic interaction may be important for cresolase inhibition (Saboury *et al.*, 2006). Understanding the role of hydrophobic and electrostatic interactions in inhibitor binding to the active site of the enzyme can lead to designing new potent inhibitors of MT. In the present investigation, the inhibitory effects of four synthesized alkyl xanthates, with different aliphatic tails, C_2, C_3, C_4 and C_6, are described and kinetic analysis of their action towards both cresolase and catecholase activities is given.

MATERIALS AND METHODS

Mushroom tyrosinase (MT; EC 1.14.18.1) from a commercially important source of *Agricus bisporus*, specific activity 3400 units/mg, was purchased from Sigma. 4-[(4-methylbenzo)azo]-1,2-benzendiol (MeBACat) (Fig. 1a) and 4-[(4-methylphenyl)azo]-phenol (MePAPh) (Fig. 1b), as synthetic substrates for the enzyme for the catecholase and cresolase reactions, respectively, were prepared as previously described (Haghbeen & Tan, 1998).

Ethyl xanthate (**I**), propyl xanthate (**II**), butyl xanthate (**III**) and hexyl xanthate (**IV**), sodium salts (Fig. 1c), were synthesized. Ethanol, 1-propanol, 1-butanol, 1-hexanol, carbon disulfide and sodium hydroxide were purchased from Merck Chemical Co. (Germany) and used as received. Infrared spectra were obtained on Nicolet 5-DXB FT-IR spectrophotometer in the range of 4000–400 cm^{-1} in KBr pellets. Microchemical analysis of carbon and hydrogen for the compounds were carried out on CHN Rapid Herause. ^1H NMR spectra were recorded on a Brucker DRX-500 Avance spectrophotometer at 500 MHz in DMSO-d_6 using sodium-3-trimethylpropionate as internal reference. ^1H NMR data are expressed in parts per million (ppm) and are reported as chemical shift position (δH), multiplicity (s=singlet, d=doublet, t=triplet, q=quartet, m=multiple) and assignment. Melting points were measured on a Unimelt capillary melting point apparatus and are reported uncorrected.

Sodium phosphate buffer (10 mM, pH 6.8) was used throughout this research and the corresponding salts were obtained from Merck. All experiments were carried out at 20°C.

Synthesis of sodium ethyl xanthate (I). This compound was prepared by an improved procedure as compared to that of literature (Mohamed *et al.*, 2004). Four grams (100 mmol) NaOH and 5.87 ml (100 mmol) ethanol were mixed in a 100 ml stoppered flask and stirred to get a homogenous curdy solution. The flask was kept in an ice bath and 20 ml of CS_2 (200 mmol) was added dropwise with constant stirring over a period of 30 min, the solution became cloudy yellow. Then the mouth of the reaction vessel was closed using a proper stopper and left to stir for 1 h in an ice bath and 2 h at room temperature. This crude product was completely dried at 35°C and powdered in a mortar. This powder was stirred with 30 ml acetone over a period of 10 min, and filtered to remove undissolved particles. To the filterate 40 ml diethylether was added and kept in refrigerator overnight. The bright yellow crystals obtained were filtered and washed twice with ether and dried at 35°C (yield 11.52 g, 80%; decomposes at 104°C). ^1H NMR (500 MHz, DMSO-d_6, ppm): 4.19 (q, O-CH_2), 1.15 (t, O-CH_2CH_3). Analytical calculated for $C_3H_5OS_2Na$: C, 25.00; H, 3.47. Analytical found: C, 25.10; H, 3.43. Solid-state IR spectroscopy of sodium ethyl xanthate showed two characteristic bands at 1127 and 1035 cm^{-1} assigned to ν_{c-o} and ν_{c-s} modes, which are similar to the other

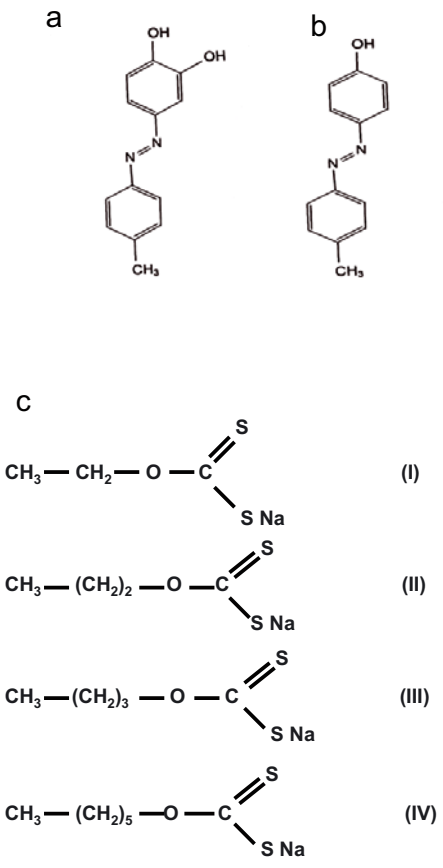

Figure 1. Chemicals used as substrates and inhibitors of MT.
4-[(4-methylbenzo)azo]-1,2-benzendiol (MeBACat) (a) and 4-[(4-methylphenyl)azo]-phenol (MePAPh) (b), used as synthetic substrates for MT for catecholase and cresolase reactions, respectively. Ethyl xanthate (**I**), propyl xanthate (**II**), butyl xanthate (**III**) and hexyl xanthate, sodium salts, (c) used as new MT inhibitors.

Table 1. Thermodynamic parameters of binding of ethyl xanthate (I), propyl xanthate (II), butyl xanthate (III) and hexyl xanthate (IV), sodium salts, to mushroom tyrosinase at 20°C and pH 6.8

Reaction type	Ligand	K_a (M^{-1})	K_i (μM)	ΔG^o (kJ/ mol)	α
Catecholase	**I**	71×10^4	1.4	−32.82	5.7
	II	20×10^4	5	−29.73	8.0
	III	7.7×10^4	13	−27.41	∞
	IV	4×10^4	25	−25.81	∞
Cresolase	**I**	7.2×10^4	13.8	−27.25	0
	II	9.09×10^4	11	−27.81	0
	III	12.5×10^4	8	−28.59	∞
	IV	20×10^4	5	−29.73	∞

K_a, association constant; K_i, inhibition constant; α, interaction factor.

xanthates reported (Fackler & William, 1969; Katsoulos & Tsipis, 1984; Mohamed *et al.*, 2004).

Synthesis of sodium propyl xanthate (II). This compound was prepared by following the procedure described for sodium ethyl xanthate except that 1-propanol (7.46 ml/100 mmol) was used instead of ethyl alcohol (yield 12.32 g, 78%; decomposes at 85°C). ^{1}H NMR (500 MHz, DMSO-d_6, ppm): 4.11 (t, O-CH_2), 1.57 (m, O-CH_2-CH_2), 0.85 (t, O-CH_2-CH_2CH_3). Analytical calculated for $C_4H_7OS_2Na$: C, 30.38; H, 4.43. Analytical found: C, 30.41; H, 4.50. Solid-state IR spectroscopy of sodium propyl xanthate showed two characteristic bands at 1175 and 1059 cm^{-1} assigned to ν_{c-o} and ν_{c-s} modes, which are similar to the other xanthates reported (Fackler & William, 1969; Katsoulos & Tsipis, 1984; Mohamed *et al.*, 2004).

Synthesis of sodium butyl xanthate (III). This compound was prepared by following the procedure described for sodium ethyl xanthate except that 1-butanol (9.15 ml, 100 mmol) was used instead of ethyl alcohol (yield 14.27 g, 83%; decomposes at 86°C ^{1}H NMR (500 MHz, DMSO-d_6, ppm): 4.37 (t, O-CH_2), 1.66 (m, O-CH_2-CH_2), 1.35 (m, O-CH_2-CH_2-CH_2), 0.86 (t, O-CH_2-CH_2-CH_2-CH_3). Analytical calculated for $C_5H_9OS_2Na$: C, 30.00; H 4.50. Analytical found: C, 30.08; H, 4.53. Solid-state IR spectroscopy of sodium buthyl xanthate showed two characteristic bands at 1169 and 1071 cm^{-1} assigned to ν_{c-o} and ν_{c-s} modes, which are similar to the other xanthates reported (Fackler & William, 1969; Katsoulos & Tsipis, 1984; Mohamed *et al.*, 2004).

Synthesis of sodium hexyl xanthate (IV). This compound was prepared by following the procedure described for sodium ethyl xanthate except that 1-hexanol (12.55 ml, 100 mmol) was used instead of ethyl alcohol (yield 15.80 g, 79%; decomposes at 208°C). ^{1}H NMR (500 MHz, DMSO-d_6, ppm): 4.15 (t, O-CH_2), 1.55 (m, O-CH_2-CH_2), 1.26 (m, O-CH_2-CH_2-CH_3), 0.85 (t, O-$(CH_2)_3$-CH_3). Analytical calculated for $C_7H_{13}OS_2Na$: C, 42.00; H, 6.50. Analytical found: C, 41.92; H, 6.53. Solid-state IR spectroscopy of sodium hexyl xanthate showed two characteristic bands at 1157 and 1074 cm^{-1} assigned to ν_{c-o} and ν_{c-s} modes, which are similar to the other xanthates reported (Fackler & William, 1969; Katsoulos & Tsipis, 1984; Mohamed *et al.*, 2004).

Kinetic measurements. Kinetic assays of catecholase and cresolase activities were carried out through depletion of MeBACat and MePAPh, respectively, for 1 and 2 min, with enzyme concentrations of 11.11 and 112.68 μg/ml, at 473 nm and 352 nm wavelengths using a Cary 100 Bio spectrophotometer, with jacketed cell holders. Freshly dissolved enzyme, substrate, **I**, **II**, **III,** and **IV** were used in this work. All enzymatic reactions were run in sodium phosphate buffer (10 mM) at pH 6.8 in a conventional quartz cell thermostated at 20±0.1°C. Substrate addition followed after incubation of enzyme with different concentrations of the n-alkyl xanthate.

RESULTS AND DISCUSSION

The inhibitory effects of four different copmpounds (xanthates) on both MT activities were examined at pH 6.8 and temperature of 20°C.

Kinetic parameters of cresolase activity of MT in the presence of I, II, III and IV

Double reciprocal Lineweaver-Burk plots for the cresolase activity of MT assayed as hydroxylation of MePAPh, in the presence of different fixed concentrations of **I**, **II**, **III** and **IV** are shown in Figs. 2–5, respectively. These plots for **I** and **II** (Figs. 2 and 3)

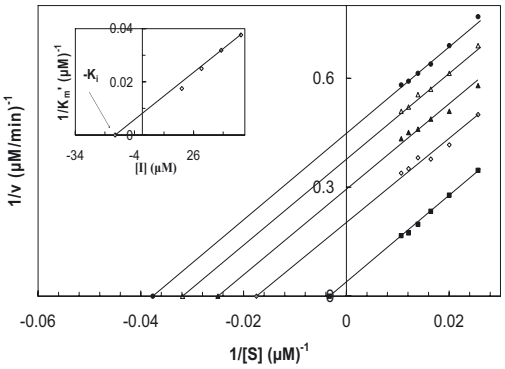

Figure 2. Double reciprocal Lineweaver-Burk plots of MT kinetics assays for cresolase reactions. MePAPh was a substrate.
The reaction was done in 10 mM sodium phosphate buffer, pH 6.8, at 20°C and 112.68 μg/ml enzyme, in the presence of different concentrations of **I**: 0 mM (■), 0.02 mM (◊), 0.03 mM (▲), 0.04 mM (Δ), 0.05 mM (●). Inset: secondary plot, $1/V_{max}'$ against different concentrations of inhibitor, which gives the inhibition constant ($-K_i$) from the abscissa-intercepts.

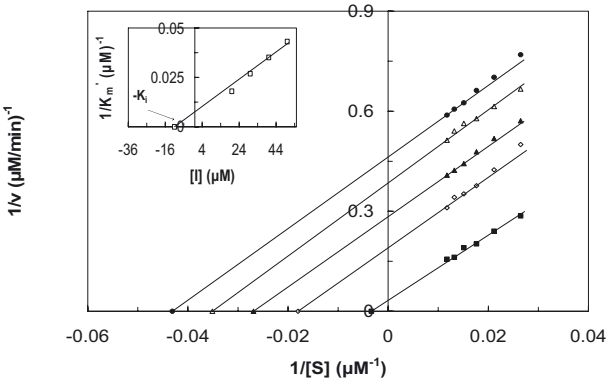

Figure 3. Double reciprocal Lineweaver-Burk plots of MT kinetic assay for cresolase reactions. MePAPh was a substrate.
The reaction was done in 10 mM sodium phosphate buffer, pH 6.8, at 20°C and 112.68 μg/ml enzyme, in the presence of different concentrations of **II**: 0 mM (■), 0.02 mM (◊), 0.03 mM (▲), 0.04 mM (Δ), 0.05 mM (●). Inset: secondary plot, $1/V_{max}'$ against different concentrations of inhibitor, which gives the inhibition constant ($-K_i$) from the abscissa-intercepts.

show a set of parallel straight lines, which intersect the x axis, which indicates uncompetitive inhibition. The apparent maximum velocity (V_{max}') and apparent Michaelis constant (K_m') values can be obtained at different fixed concentrations of each inhibitors (**I** and **II**). A secondary plot of $1/V_{max}'$ against the concentration of inhibitor gives a straight line with the abscissa-intercept of $-K_i$ (see the insets of Figs. 2 and 3), where K_i is the inhibition constant. Double reciprocal Lineweaver-Burk plots for **III** and **IV** give a set of straight lines intersecting exactly on the vertical axis, the value of maximum velocity (V_{max}) is unchanged by the inhibitors but the K_m' values are increased, which indicates competitive inhibition for both **III** and **IV** (see Figs. 4 and 5). The insets in Figs. 4 and 5 show the secondary plot, the K_m' at given concentration of inhibitors (**III** and **IV**) *versus* the concentration of inhibitors, which give the inhibition constants ($-K_i$) from the abscissa-intercepts.

Results for K_i values of cresolase activity of MT in the presence of **I**, **II**, **III** and **IV** are summarized in Table 1. **I** and **II** can bind to the enzyme–substrate complex only. Binding of the substrate is required for the binding of the inhibitor, which

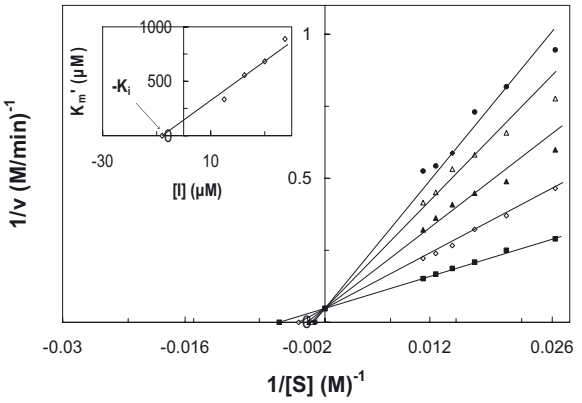

Figure 4. Double reciprocal Lineweaver-Burk plots of MT kinetic assay for cresolase reactions.
MePAPh was a substrate. The reaction was done in 10 mM sodium phosphate buffer, pH 6.8, at 20°C and 112.68 μg/ml enzyme, in the presence of different concentrations of **III**: 0 mM (■), 0.015 mM (◊), 0.0225 mM (▲), 0.03 mM (Δ), 0.0375 mM (●). Inset: secondary plot, the K_m' against different concentrations of inhibitor, which gives the inhibition constant ($-K_i$) from the abscissa-intercepts.

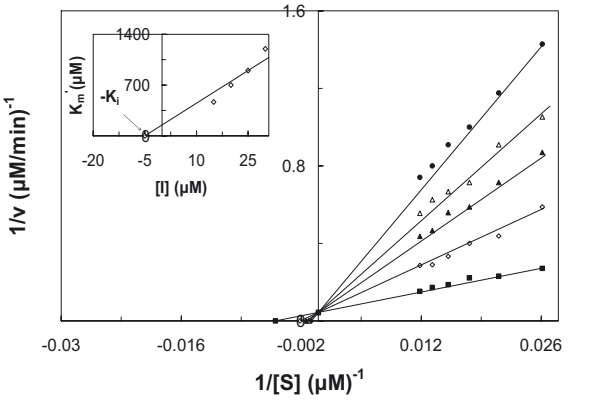

Figure 5. Double reciprocal Lineweaver-Burk plots of MT kinetic assay for cresolase reactions. MePAPh was a substrate.
The reaction was done in 10 mM sodium phosphate buffer, pH 6.8, at 20°C and 112.68 μg/ml enzyme, in the presence of different concentrations of **IV**: 0 mM (■), 0.015 mM (◊), 0.02 mM (▲), 0.025 mM (Δ), 0.03 mM (●). Inset: secondary plot, the K_m' against different concentrations of inhibitor, which gives the inhibition constant ($-K_i$) from the abscissa-intercepts.

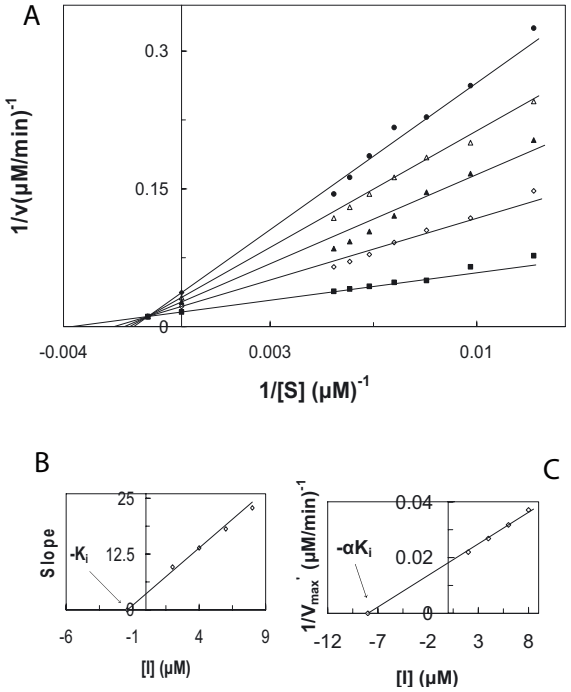

Figure 6. Double reciprocal Lineweaver-Burk plots of MT kinetic assay for catecholase reactions. MeBACat was a substrate.

(**A**) The reaction was done in 10 mM sodium phosphate buffer, pH 6.8, at 20°C and 11.11 μg/ml enzyme, in the presence of different concentrations of **I**: 0 mM (■), 0.004 mM (◊), 0.008 mM (▲), 0.012 mM (Δ), 0.016 mM (●). (**B**) Secondary plot of the slope against the concentration of inhibitor, which gives $-K_i$ from the abscissa-intercept. (**C**) Secondary plot of $1/V_{max}'$ at given concentration of inhibitor *versus* concentration of inhibitor, which gives $-\alpha K_i$ from the abscissa-intercepts.

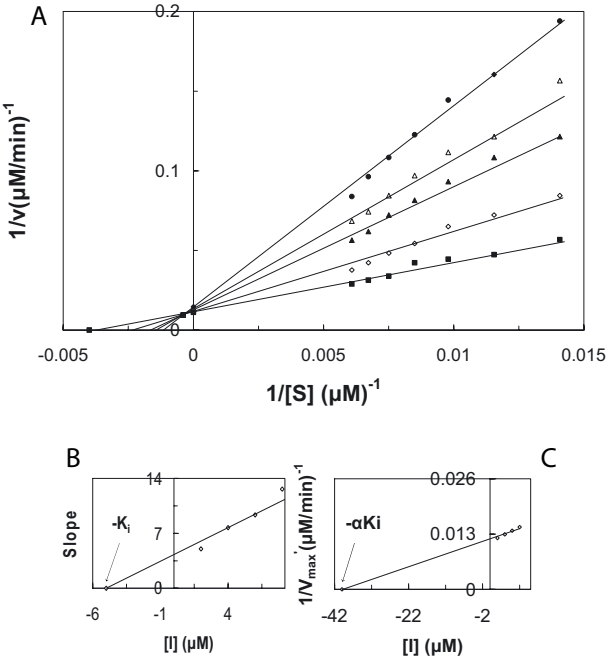

Figure 7. Double reciprocal Lineweaver-Burk plots of MT kinetic assay for catecholase reactions. MeBACat was a substrate.

(**A**)The reaction was done in 10 mM sodium phosphate buffer, pH 6.8, at 20°C and 11.11 μg/ml enzyme, in the presence of different concentrations of **II**: 0 mM (■), 0.004 mM (◊), 0.008 mM (▲), 0.012 mM (Δ), 0.016 mM (●). (**B**) Secondary plot of the slope against the concentration of inhibitor, which gives $-K_i$ from the abscissa-intercept. (**C**) Secondary plot of $1/V_{max}'$ at given concentration of inhibitor *versus* concentration of inhibitor, which gives $-\alpha K_i$ from the abscissa-intercepts.

means that there is an infinite cooperativity between the two binding sites of substrate and inhibitor. But **III** and **IV** bind to the substrate-binding site and inhibit the cresolase activity in the competitive mode. Adding $-CH_2-$ groups leads to competitive inhibition for **III** and **IV** with an infinite value of α, which means that the interaction between the substrate and the inhibitor binding sites is so high that only either substrate or inhibitor can bind to the enzyme. As shown in Table 1, the highest value of K_i is for **I** (13.8 μM) and the lowest for **IV** (5 μM). So the affinity of the inhibitor for the enzyme changes slightly in the order of **I<II<III<IV**. Increasing the size of the hydrophobic tail of the inhibitor by adding $-CH_2-$ groups leads to the binding of the inhibitor to free enzyme and also the affinity of the binding is slightly increased.

Kinetic parameters of catecholase activity of MT in the presence of I, II, III and IV

Double reciprocal Lineweaver-Burk plots for the catecholase activity of MT assayed as oxidation of MeBACat in the presence of different fixed concentrations of **I**, **II**, **III** and **IV** are shown in Figs. 6a, 7a, 8 and 9, respectively. These plots show a set of straight lines which intersect on the left-hand side of the vertical axis, near the horizontal axis for **I** (Fig. 6a) and a little closer to the horizontal axis for **II** (Fig. 7a), which indicates mixed inhibition. The apparent maximum velocity (V_{max}') and apparent Michaelis constant (K_m') values as well as the slope values of these straight lines (K_m'/V_{max}') can be obtained at different fixed concentrations of each inhibitor (**I** and **II**). A secondary plot of the slope against the concentration of inhibitor gives a straight line with the abscissa-intercept of $-K_i$ (see Figs. 6b and 7b for **I** and **II**, respectively). Another secondary plot of the reciprocal apparent maximum velocity against the concentration of inhibitor gives a straight line with the abscissa-intercept of $-\alpha K_i$ (see Figs. 6c and 7c for **I** and **II**, respectively), where K_i is the inhibition constant and α is the interaction factor between the substrate and inhibitor sites. Double reciprocal Lineweaver-Burk plot for **III** and **IV** give a set of straight lines intersecting exactly on the verti-

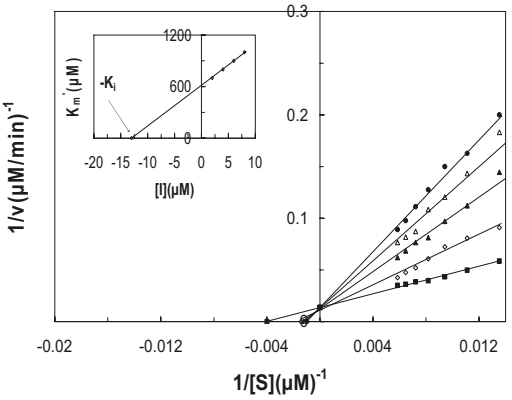

Figure 8. Double reciprocal Lineweaver-Burk plots of MT kinetic assay for catecholase reactions. MeBACat was a substrate.
The reaction was done in 10 mM sodium phosphate buffer, pH 6.8, at 20ºC and 11.11 μg/ml enzyme, in the presence of different concentrations of **III**: 0 mM (■), 0.002 mM (◊), 0.004 mM (▲), 0.006 mM (Δ), 0.008 mM (●). Inset: secondary plot, the K_m' against different concentrations of inhibitor, which gives the inhibition constant ($-K_i$) from the abscissa-intercepts.

cal axis, the values of maximum velocity (V_{max}) are unchanged by the inhibitors but the K_m' values are increased, indicating competitive inhibition for **III** and **IV** (see Figs. 8 and 9). The insets in Figs. 8 and 9 show the secondary plots, the K_m' at given concentration of inhibitors (**III** and **IV**) *versus* the concentration of the inhibitors, which give the inhibition constants ($-K_i$) from the abscissa-intercepts.

Results for the K_i and α values of the catecholase activity of MT in the presence of **I**, **II**, **III** and **IV** are summarized in Table 1. The α values for **I** and **II** are 5.7 and 8.0, respectively. It means that the negative cooperativity between substrate and inhibitor is increased due to the addition of a $-CH_2-$ group to the molecular structure of the ligand. Adding subsequent $-CH_2-$ groups leads to competitive inhibition for **III** and **IV** with an infinite value for α, which means that the interaction between the substrate and inhibitor binding sites is so high that only either substrate or inhibitor can bind to the enzyme. As shown in Table 1, the highest value of K_i is for **IV** (25 μM) and the lowest for **I** (1.4 μM). The affinity of inhibitor binding to the enzyme is in the order of **IV<III<II<I.** Extending the size of the inhibitor molecule by adding a $-CH_2-$ group causes more negative cooperativity in the binding sites of substrate and inhibitor, but the affinity of the binding is decreased.

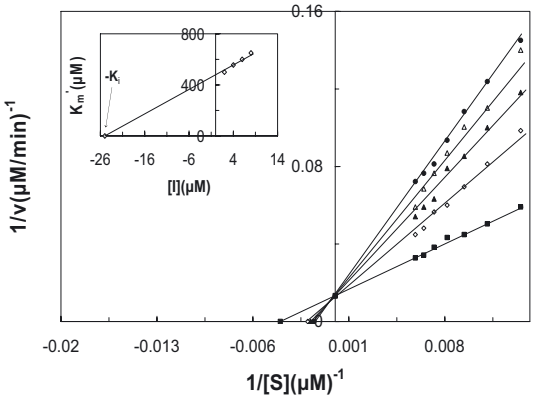

Figure 9. Double reciprocal Lineweaver-Burk plots of MT kinetic assay for catecholase reactions. MeBACat was a substrate.
The reaction was done in 10 mM sodium phosphate buffer, pH 6.8, at 20ºC and 11.11 μg/ml enzyme, in the presence of different concentrations of **IV**: 0 mM (■), 0.002 mM (◊), 0.004 mM (▲), 0.006 mM (Δ), 0.008 mM (●). Inset: secondary plot, the K_m' against different concentrations of inhibitor, which gives the inhibition constant ($-K_i$) from the abscissa-intercepts.

The change of the standard Gibbs free energy of binding (ΔG^o) for each inhibitor was calculated using the association binding constant (K_a), obtained from the inverse of the K_i value, in the equation $\Delta G^o = -RT \ln K_a$; where R is the gas constant and T is the absolute temperature (Atkins & dePaula, 2002). The calculated ΔG^o values of the four ligands for the cresolase and catecholase activities are summarized in Table 1. The inhibitor binding process is spontaneous ($\Delta G^o<0$) in all cases.

It has been reported that thiol compounds can act as inhibitors of tyrosinase due to their ability to chelate Cu^{+2} (Hanlon & Shuman, 1975). All our four synthesized compounds also acted as inhibitors. Each n-alkyl xanthate produces an anion with a head group of S^- and a hydrophobic tail. The size of the hydrophobic tail is more important in catecholase inhibition, than in cresolsae inhibition, due to the more diverse K_i values in catecholase inhibition. Hence, hydrophobic interactions have a more important role in catecholase inhibition than in cresolase inhibition. Moreover, the K_i values for catecholase inhibition increase as the length of the hydrophobic tail increases for these compounds, which means that a shorter tail gives a more potent inhibitor; however, it is the opposite for cresolase inhibition. Hydrophobic interactions between the tail of the ligand and the hydrophobic pockets in the active site of the enzyme reduce the affinity of the inhibitor binding in catecholase inhibition. The cresolase activity occurs when the enzyme is in the oxy form and the catecholase activity occurs when the enzyme is in the met form, thus it seems likely that the hydrophobic pockets in the oxy form are different from those in the met form. The structure of the hydrophobic pockets of the enzyme is energetically favorable for binding of an inhibitor that has a shorter hydrophobic chain in the catecholase activity. Our results may assist future attempts to design inhibitors that could be used to prevent un-

desirable fruit browning or as color skin modulators in mammals.

Acknowledgements

The financial support given by the University of Tehran and the Iran National Science Foundation (INSF) are gratefully acknowledged.

REFERENCES

Andrawis A, Khan V (1996) Effect of methimazole on the activity of mushroom tyrosinase. *Biochem J* **35**: 91–96.

Atkins P, dePaula J (2002) Physical Chemistry, 7th edn, chapter 9. W. H. Freeman & Company, NewYork.

Barrett FM (1984) Wound-healing phenoloxidase in larval cuticle of *Calpodes ethlius* (Lepidoptera: Hesperiidae). *Can J Zool* **62**: 834–838.

Battaini G, Monzani E, Casella L, Santagostini L, Pagliarin R (2000) Inhibition of the catecholase activity of biomimetic dinuclear copper complexes by kojic acid. *J Biol Inorg Chem* **5**: 262–268.

Cabanes J, Chazarra S, Garcia-Carmona F (1994) Kojic acid, a cosmetic skin agent, is a slow-binding inhibitor of catecholase activity of tyrosinase. *J Pharm Pharmacol* **46**: 982–985.

Chen JS, Wei C, Marshall MR (1991a) Inhibition mechanism of kojic acid on polyphenol oxidase. *J Agric Food Chem* **39**: 1897–1901.

Chen JS, Wei C, Rolle RS, Otwell WS, Balban MO, Marshall MR (1991b) Inhibitory effect of kojic acid on some plant and crustacean polyphenol oxidases. *J Agric Food Chem* **39**: 1396–1401.

Chen QX, Kubo I (2002) Kinetics of mushroom tyrosinase inhibition by quercetin. *J Agric Food Chem* **50**: 4108–4112.

Espin JC, Wichers HG (2001) Effect of captopril on mushroom tyrosinase activity *in vivo. Biochim Biophys Acta* **1554**: 289–300.

Fackler JP Jr, William CS (1969) Sulfur ligand complexes. IX. Reactions of metal xanthates and their derivatives. The formation of biophosphine-dithiocarbonate and –trithiocarbonate complexes of palladium (II) and platinum (II). *Inorg Chem* **8**: 1631–1639.

Ferrar PH, Walker JRI (1996) Inhibition of diphenoloxidases: a comparative study. *J Food Biochem* **20**: 15–30.

Gheibi N, Saboury AA, Haghbeen K, Moosavi-Movahedi AA (2005) Activity and structural changes of mushroom tyrosinase induced by n-alkyl sulfates. *Colloids Surface B: Biointerfaces* **45**: 104–107.

Gheibi N, Saboury AA, Mansury-Torshizy H, Haghbeen K, Moosavi-Movahedi AA (2004) The inhibition effect of some n-alkyl dithiocarbamates on mushroom tyrosinase. *J Enz Inhib Med Chem* **20**: 393–399.

Goetghebeur M, Kermasha S (1996) Inhibition of polyphenol oxidase by copper-metallothionein from *Aspergillus niger*. *Phtochemistry* **42**: 935–940.

Haghbeen K, Saboury AA, Karbassi F (2004) Substrate share in the suicide inactivation of mushroom tyrosinase. *Biochim Biophys Acta* **1675**: 139–146.

Haghbeen K, Tan EW (1998) Facile synthesis of catechol azo dyes. *J Org Chem* **63**: 4503–4505.

Hanlon DP, Shuman S (1975) Copper ion binding and enzyme inhibitory properties of the antithyroid drug methimazole. *Experientia* **31**: 1005–1006.

Hepp AF, Himmelwright RS, Eickman NC, Solomon EI (1979) Ligand displacement reactions of oxyhemocyanin: comparison of reactivities of arthropods and mollusks. *Biochem Biophys Res Commun* **89**: 1050–1057.

Himmelwright RS, Eickman NC, Solomon EI (1979) Reactions and interconversion of met and dimer hemocyanin. *Biochem Biophys Res Commun* **86**: 628–634.

Himmelwright RS, Eickman NC, Lubein CD, Solomon EI (1980) Chemical and spectroscopic comparison of the binuclear copper active site of ollusk and arthropod hemocyanins. *J Am Chem Soc* **102**: 5378–5388.

Jackman MP, Hajnal A, Lerch K (1991) Albino mutants of *Streptomyces glaucescens* tyrosinase. *Biochem J* **274**: 707–713.

Kahn V (1995) **Title!** In *Enzymatic Browning and its Prevention* (Lee CY, Whitaker JR, eds) pp 277–294, American Chemical Society, Washington DC.

Kahn V, Ben-Shalom N, Zakin V (1997) Effect of kojic acid on the oxidation of *N*-acetyldopamine by mushroom tyrosinase. *J Agric Food Chem* **45**: 4460–4465.

Karbassi F, Haghbeen K, Saboury AA, Ranjbar B, Moosavi-Movahedi AA (2003) Activity, structural and stability changes of mushroom tyrosinase by sodium dodecyl sulfate. *Colloids Surface B: Biointerfaces* **32**: 137–143.

Karbassi F, Haghbeen K, Saboury AA, Ranjbar B, Moosavi-Movahedi AA, Farzami B (2004a) Stability, structural and suicide inactivation changes of mushroom tyrosinase after acetylation by *N*-acetylimidazole. *Int J Biol Macromol* **34**: 257–262.

Karbassi F, Saboury AA, Hassan Khan MT, Iqbal Choudhary M, Saifi ZS (2004b) Mushroom tyrosinase inhibition by two potent uncompetitive inhibitors. *J Enz Inhib Med Chem* **19**: 349–353.

Katsoulos GA, Tsipis CA (1984) Synthesis of some novel Pt (II) and Pd (II) n-alkyliminodithiocarbonato complexes and investigation of the mechanism of their formation by CNDO/2 quantum chemical calculations. *Inorg Chim Acta* **84**: 89–94.

Kim YM, Yun J, Lee CK, Lee H, Min KR, Kim Y (2002) Oxyresveratrol and hydroxystilbene compounds: inhibitory effect on tyrosinase and mechanism of action. *J Biol Chem* **227**: 16340–16344.

Kim YJ, Chung JE, Kurisawa M, Uyama H, Kobayashi S (2004) New tyrosinase inhibitors, (+)-catechin-aldehyde polycondensates. *Biomacromolecules* **5**: 474–479.

Kubo I, Kinst-Hori I (1988) Tyrosinase inhibitors from cumin. *J Agric Food Chem* **46**: 5338–5341.

Kubo I, Kinst-Hori I, Ishiguro K, Chaudhuri SK, Sanchez Y, Ogura T (1994) Tyrosinase inhibitory flovonoids from *Heterotheca inuloides* and their structural functions. *Bioorg Med Chem Lett* **4**: 1443–1446.

Kubo I, Kinst-Hori I (1999) Flovonols from saffron flower: tyrosinase inhibitory activity and inhibition mechanism. *J Agric Food Chem* **47**: 4121–4125.

Kubo I, Kinst-Hori I, Chaudhuri SK, Kubo Y, Sanchez Y, Ogura T (2000) Flovonols from *Heterothesca inuloides*: tyrosinase inhibitory activity and structural criteria. *Bioorg Med Chem* **8**: 1749–1755.

Lee HS (2002) Tyrosinase inbibitors of pulsatilla cernua root-derived materials. *J Agric Food Chem* **50**: 1400–1403.

Lee SE, Kim MK, Lee SG, Ahn YJ, Lee HS (2000) Inhibition effects of cinnamomum cassia bark-derived materials on mushroom tyrosinase. *Food Sci Biotechnol* **9**: 330–333.

Lerch K (1981) In *Metal Ions in Biological Systems* (Sigel H, ed) pp 143–186, Marcel Dekker, New York.

Liangli YU (2003) Inhibitory effects of (S)- and I-6–hydroxy-2,5,7,8–tetramethylchroman-2–carboxylic acids on tyrosinase activity. *J Agric Food Chem* **51**: 2344–2347.

Lim JT (1999) Treatment of melasma using kojic acid in a gel containing hydroquinone and glycolic acid. *Dermatol Surg* **25**: 282–284.

Maeda K, Fukuda M (1991) *In vitro* effectiveness of several whitening cosmetic components in human melanocytes. *J Soc Cosmet Chem* **42**: 361–368

Martinez MV, Whitaker JR (1995) The biochemistry and control of enzymatic browning. *Trends Food Sci Technol* **6**: 195–200.

Mohamed AA, Kani I, Ramirez AO, Fackler JP (2004) Synthesis, characterization and luminescent properties of dinuclear gold(I) xanthate complexes: X-ray structure of $[Au_2(n\text{-Bu-xanthate})_2]$. *Inorg Chem* **43**: 3833–3839.

Mosher DB, Pathak MA, Fitzpatric TB eds (1983) *Update: dermatology in general medicine*. pp 205–225; McGraw Hill, New York.

Pawelek JM, Korner AM (1982) The biosynthesis of mammalian melanin. *J Am Chem Soc* **70**: 136–145.

Saboury AA, Zolghadri S, Haghbeen K, Moosavi-Movahedi AA (2006) The inhibitory effect of benzenethiol on the cresolase and catecholase activities of mushroom tyrosinase. *J Enz Inhib Med Chem* **21**: in press.

Sanchez-Ferrer A, Rodriguez-Lopez JN, Garcia-Canovas F, Garcia-Carmona F (1995) Tyrosinase: a comprehensive review of its mechanism. *Biochim Biophys Acta* **1247**: 1–11.

Schoot Uiterkamp AJM (1972) Monomer and magnetic dipole-coupled Cu^{+2} EPR signals in nitrosylhemocyanin. *FEBS Lett* **20**: 93–96.

Shareefi Borojerdi S, Haghbeen K, Karkhane AA, Fazli M, Saboury AA (2004) Successful resonance Raman study of cresolase activity of mushroom tyrosinase. *Biochem Biophys Res Commun* **314**: 925–930.

Strothkemp KJ, Jolley RL, Mason Hs (1976) Quaternary structure of mushroom tyrosinase. *Biochem Biophys Res Commun* **70**: 519–524.

Sugumaran M (1988) Molecular mechanism for cuticular sclerotization. *Adv Insect Physiol* **21**: 179–231.

Whitaker JR (1995) Polyphenol oxidase. In *Food enzymes: structure and mechanism* (Wong DWS, ed) pp 271–307, Chapman & Hall, New York.

Wilcox DE, Porras AG, Hwang YT, Lerch K, Winkler ME, Solomon E8I (1985) Substrate analogue binding to the coupled binuclear copper active site in tyrosinase. *J Am Chem Soc* **107**: 4015–4027.

Xie LP, Chen QX, Huang H, Wang HZ, Zhang RQ (2003) Inhibitory effects of some flavonoids on the activity of mushroom tyrosinase. *Biochemistry (Mosc)* **68**: 487–491.

Xu Y, Stokes AH, Freeman WM, Kumer SC, Vogt BA, Vrana KE (1997) Tyrosinase mRNA is expressed in human substantia nigra. *Mol Brain Res* **45**: 159–162.

Yong G, Leone C, Strothkemp KJ (1990) *Agricus bisporus* metapotyrosinase: preparation, characterization, and conversion to mixed-metal derivatives of the binuclear site. *Biochemistry* **29**: 9684–9690.

Zawistowski J, Biliaderis CG, Eskin NAM (1991) Polyphenol oxidase. In *Oxidative enzymes in foods* (Robinson DS, Eskin NAM, eds) pp 217–273, Elsevier Applied Science: New York.